# A new generation of spectrometers for radio astronomy: fast Fourier transform spectrometer

Bernd Klein, Sabine D. Philipp, Rolf Güsten, Ingo Krämer, Dorothea Samtleben

Bernd Klein, Sabine D. Philipp, Rolf Güsten, Ingo Krämer, Dorothea Samtleben, "A new generation of spectrometers for radio astronomy: fast Fourier transform spectrometer," Proc. SPIE 6275, Millimeter and Submillimeter Detectors and Instrumentation for Astronomy III, 627511 (27 June 2006); doi: 10.1117/12.670831

SPIE.

Event: SPIE Astronomical Telescopes + Instrumentation, 2006, Orlando, Florida , United States

# A new generation of spectrometers for radio astronomy: Fast Fourier Transform Spectrometer

Bernd Klein, Sabine D. Philipp, Rolf Güsten, Ingo Krämer and Dorothea Samtleben

Max-Planck-Institut für Radioastronomie, Auf dem Hügel 69, 53121 Bonn, Germany

## ABSTRACT

We present a new generation of very flexible and sensitive spectrometers for radio astronomical applications: Fast Fourier Transform Spectrometer (FFTS). The rapid increase in the sampling rate of commercially available analog-to-digital converters (ADCs) and the increasing power of field programmable gate array (FPGA) chips has led to the technical possibility to directly digitize the down-converted intermediate-frequency signal of coherent radio receivers and to Fourier transform the digital data stream into a power spectrum in continuous real-time with no gaps in the data. In the last years FPGAs have become very popular for building fast and reconfigurable hardware. State-of-the-art chips include several hundred dedicated 18 bit × 18 bit multipliers, which allow up to 80 billion multiplication and nearly 500 billion 36-bit additions per second. This extremely high computing power makes it now possible to implement real-time FFTs to decompose a 1 GHz frequency band into 16384 spectral channels. In this paper we present the technological concept and results of our novel broad-band 1 GHz FFTS with 16k frequency channels, which is installed at the APEX telescope. This backend can be considered prototypical for spectrometer developments for future radio astronomical applications.

**Keywords:** spectroscopy, spectrometers, Fourier transform, FFT, FPGA, radio astronomy

## 1. INTRODUCTION

Spectroscopy allows studies of the physics and chemistry of astronomical objects such as planetary atmospheres, circumstellar envelopes and the interstellar medium of our Milky Way and external galaxies. In particular submillimeter heterodyne spectroscopy allows for new insights into the very nature of these objects, since galaxies emit the bulk of their line emission and continuum at millimeter through long Far-IR wavelengths. To study, for example, interacting galaxies in the local universe or young galaxies undergoing phases of star formation, wide bandwidth spectroscopy is required. On the other hand, to study the interstellar medium in our galaxy or galaxies close-by, one wants to perform line surveys or studies of spectra of relatively complex kinematic and morphological superpositions of emissions and absorptions that requests high spectral resolution over wide bandwidths (sect. 5). Until recently, spectrographs offer usable instantaneous bandwidth from a few MHz up to 1-2 GHz with a few thousand spectral channels capable of resolving narrow spectral lines e.g. of masers or thermal line emission of gaseous clouds.

Particularly for the new APEX* sub-millimeter telescope[1], which operates at sky frequencies of several 100 GHz up to 1.5 THz, a large bandwidth is very important to allow e.g. for studies of broader lines also at the highest frequencies.

The novel FPGA-based FFTSs offer new perspectives: State-of-the-art FPGAs include several hundred dedicated $18 \times 18$ bit multipliers which allow up to $8 \times 10^{10}$ multiplications and nearly $5 \times 10^{11}$ 36-bit additions per second, giving these FPGA chips over ∼50 times higher performance in digital signal processing than the latest Intel Pentium 4 processors. By parallelization of single processing threads and using the FFT algorithm in a pipelined manner, it becomes possible to implement 16k-point Fourier transforms for input data rates up to 2 GBytes/s.

In this paper we describe the hardware and the FPGA signal processing of the FFTS developed for APEX. After a short review of common spectrometer techniques in radio astronomy (Sect. 2), we outline in Sect. 3 the

Contact information: Bernd Klein, E-mail: bklein@MPIfR-Bonn.MPG.de, phone: +49 228 525 286

*APEX is a collaboration between the Max-Planck-Institut für Radioastronomie, the European Southern Observatory, and the Onsala Space Observatory.

Millimeter and Submillimeter Detectors and Instrumentation for Astronomy III,
edited by Jonas Zmuidzinas, Wayne S. Holland, Stafford Withington, William D. Duncan,
Proc. of SPIE Vol. 6275, 627511, (2006) · 0277-786X/06/$15 · doi: 10.1117/12.670831

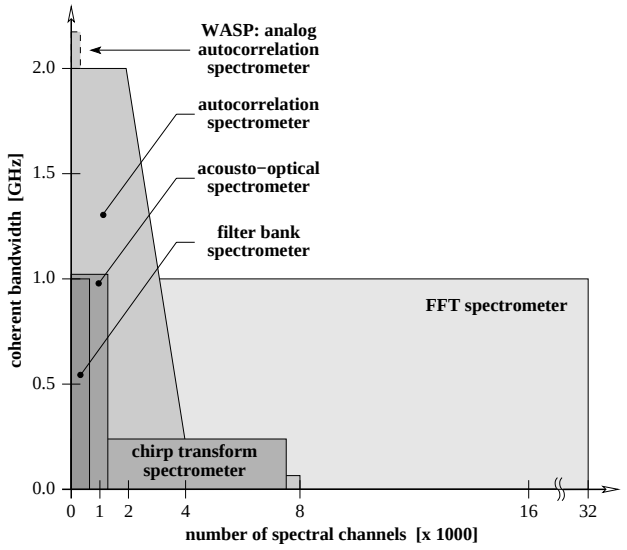


**Figure 1.** Comparison of different spectrometer types in terms of coherent bandwidth and spectral channel number applied in radio astronomy. Only FFT spectrometers provide both wide bandwidths and an impressive number of spectral channels, thus high frequency resolution.

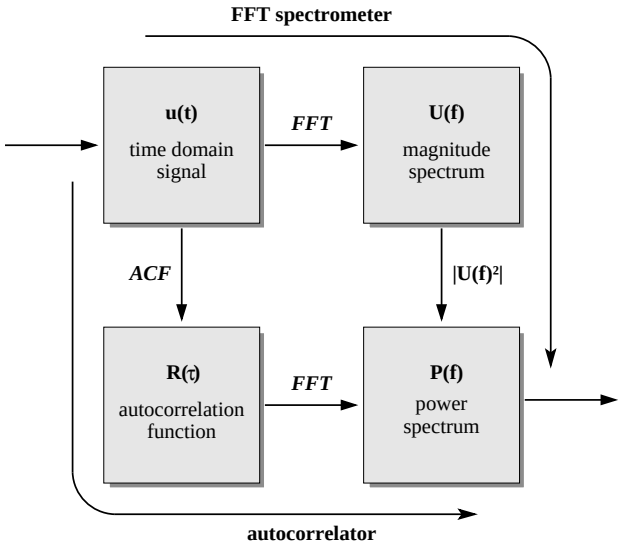


**Figure 2.** Visualization of the Wiener-Khinchin-Theorem, which states that the energy spectral density of a function is the Fourier Transform of the corresponding autocorrelation sequence.

technical design and the processing pipeline of the FFTS. Also we outline where we see possibilities for future hardware and software progresses. Sections 4 and 5 present the performance parameters and some selected spectra observed with the new FFTS at the APEX telescope.

## 2. SPECTROMETERS FOR RADIO ASTRONOMY

Because commercially available spectrum analyzers use frequency sweepers to obtain a broad-band spectrum, they are not sensitive enough for radio astronomical applications. Therefore, dedicated instruments have been developed for coherent spectral analysis. For radio frequencies one can identify four basic types of spectrometers: analog filter banks, acousto-optical spectrometers (AOS), chirp transform spectrometers (CTS), and autocorrelators (Figure 1).
Early on, spectrometers were build using analog (bandpass) filters and detectors, which were then assembled into filterbanks. Later, acousto-optical spectrometers were developed which allowed for wider bandwidth and a larger number of spectral channels[2]. AOSs currently cover bandwidths to about 1 GHz with approximately 1000 spectral channels in a compact package that requires little power[3]. Due to their design they need a stable, thermally controlled environment, which puts tight constraints on their operability.

Before the novel FFTSs became available, high resolution spectroscopic observations with many thousands of spectral channels were only possible with Chirp Transform Spectrometer[4,5]. This kind of spectrometer is capable of providing a few thousand frequency channels at moderate bandwidths of ∼200 MHz. CTS are based on the velocity dispersion of sonic surface waves, which are controlled by microstructures on the surfaces of defined crystals[6]. The dispersion properties allow the calculation of real-time convolutions, which is the fundamental function for a time-to-frequency transform.

The most commonly used spectrometers are digital autocorrelators[7] (AC). Their technology is based on the Wiener-Khinchin-Theorem, stating that the power spectrum of a signal is the Fourier transform of its autocorrelation function (ACF), as illustrated in Figure 2. The advantage of this indirect method is the possibility of accumulating the ACF even before the Fourier transform produces the final power spectrum, which reduces the number of computations and enables the calculation of the FFT in the early days. The ACF is computed by multiplication of the periodically time-shifted signals, followed by a summation of these. Limiting the sampler resolution to 1 or 2 bits, these three operations (shift, multiplication, addition) can be reduced to simple logical

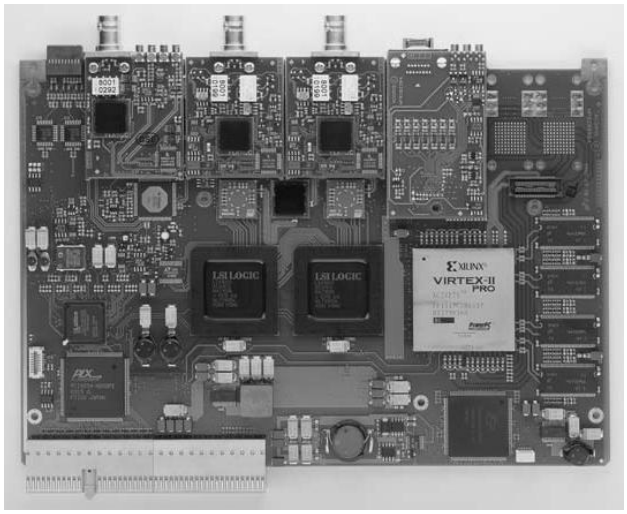

**Figure 3.** Photo of the AC240 digitizer board. The AC240 is a dual-channel 6U CompactPCI/XI digitizer with an on-board real time processing unit. The picture shows on top the two analog inputs for the signal at intermediate frequency (DC-1 GHz), an input for trigger and/or clock, and the system control interface. The FPGA processing unit is visible on the right side, and the PCI bus for data output is shown at the bottom left (`www.acqiris.com`).

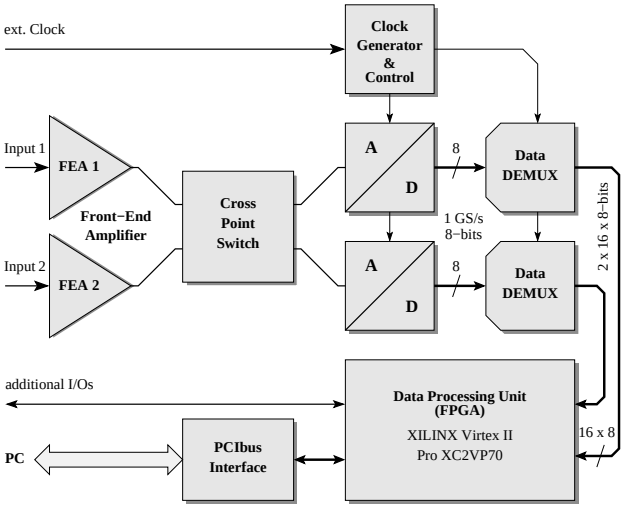


**Figure 4.** Block diagram of Acqiris' AC240 digitizer/analyzer board, the main hardware of the APEX FFT spectrometer. By applying interleaved techniques, the two 1 GS/s 8-bits ADCs can be combined to one 2 GS/s converter. To feed the high data rate output of the ADCs (2 GBytes/s) to the FPGA, de-multiplexers (DEMUX) are used which split the two 8-bits data streams at 1 GHz to $2\times16$ streams at 62.5 MHz, suitable for the FPGA.

elements, and the ACF can be integrated in a customized silicon chip. This reduction to 1 or 2 bit (mostly 3-level) data sampling, however, results in a reduced sensitivity. Nevertheless, ACs have until recently been the only way to make it possible to compute of CPU intensive Fourier transforms, so that bandwidths of order 1 GHz were achieveable[8,9]. To overcome the limit in bandwidth of digital autocorrelators, wide-band analog correlators (e.g. WASP) have been developed. WASP bypass the fast sampler problem of digital ACs by shifting all high-speed processing to the analog electronics. The (auto-)correlation function is calculated by a combination of transmission line delays and direct voltage multiplication in transistor mixers. Today, analog correlators achieve coherent bandwidths of 4 GHz and more with 128 lags, which correspond to 128 spectral channels[10,11].
A comparison of different spectrometers in terms of instantaneous bandwidth and number of spectral channel is shown in Figure 1.

## 3. DEVELOPMENT OF THE APEX FFTS

The rapid increase in the sampling rate of commercially available analog-to-digital converters (ADCs) and the increasing power of field programmable gate arrays (FPGAs) chips has led to the possibility to directly digitize the down-converted intermediate frequency (IF) signals of coherent radio-receivers, and to transform the digital signal into a spectrum in real-time. Based on the technological progress and the experiences gained in building a narrow-band FFTS[12], the APEX FFTS[13] was developed by the MPIfR Digital Group.

### 3.1. FFTS: Hardware

The APEX FFTS is based on the currently most powerful digitizer/analyzer board (AC240, Fig. 3) available from Acqiris[†], Switzerland. It incorporates two 1 GS/s ADCs which feed a XILINX VirtexII Pro70 FPGA chip (Fig. 4). By combining both ADCs in an interleave manner (180 deg phase-shift), the AC240 is capable of sampling an analog input signal at 2 GHz clock rate which results in a 1 GHz Nyquist bandwidth. The accurate interleave adjustment (calibration) of both ADCs is realized by a control circuit and an on-board clock generator.

[†] `www.acqiris.com`

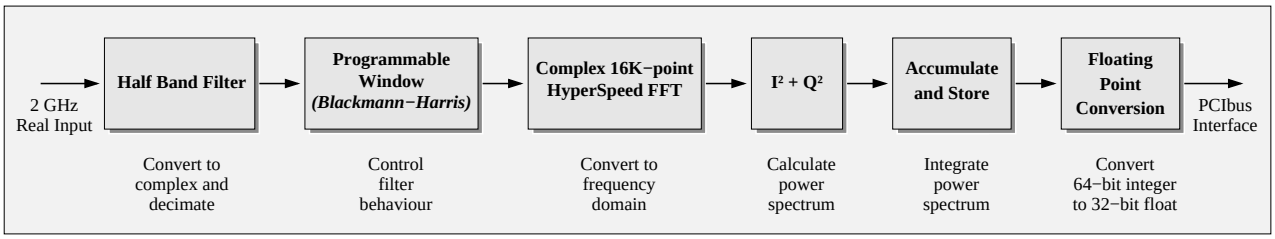


**Figure 5.** Block diagram of the RF Engines 2 GHz Spectrometer Core for FPGA, as described in section 3.2

The sample rate for both ADCs is selectable by software in a 1, 2, 2.5, 4 and 5 sequence, resulting in 100 MS/s to 2 GS/s. For multi-board applications which need a synchronized sampling, the time base of the clock generator can be driven from an external reference frequency. The AC240's 50 Ω signal inputs feature programmable front-end electronics with input voltage ranges selectable in 7 steps from 50 mV to 5 V and variable voltage offsets. The board allows both AC and DC input signal coupling. In addition, a programmable trigger-input enables an external start of sampling and data processing. The AC240 is designed as a standard 6U compact PCI/PXI board. Processed digitized data can be transfered, in DMA-mode, directly to the host PC via the PCIbus at sustained rates of up to 100 MB/s. For a more detailed description of the AC240 Board, we refer to the Acqiris documentation[†]. A very similar FFTS using the same AC240 Board is presented in[14].

### 3.2. FFTS: Signal processing pipeline

The digital signal conversion from the time domain to an integrated power spectrum is done in only one complex FPGA chip. The spectrometer core development was contracted to RF Engines Ltd. (RFEL), following our guidelines, and was finally integrated at MPIfR. The core is based on RFEL's HyperSpeed Fast Fourier Transform (FFT) technology. It receives 8-bit samples from the two ADCs at a continuous sample rate of 2 GHz and then processes this data in a sequence of four steps, as indicated in the flow of Figure 5: First, a Digital Half Band Filter (DHBF) converts the input samples to a complex I/Q-format and reduces the sample rate by a factor of two (decimation), which eases the subsequent processing requirements. A useful side effect of the DHBF is its ability to reduce the level on both bandpass sides. Indeed, this limits the useable bandwidth to ∼900 MHz but has the great advantage of decreasing aliasing effects caused by real analog filters with finite stop band rejection. The DHBF is followed by the application of a windowing function, which weights the data in order to control the filtering performance of the FFT. The coefficients are user programmable at run-time, allowing the performance characteristics of the spectrometer to be modified for changing operational scenarios. For a high resolution and high dynamic-range spectrometer, a 3-term Blackman-Harris window is a good compromise between sidelobe reduction, sidelobe fall-off and main-lobe widening. For a comprehensive discussion about window functions and their properties, the interested reader is refered to[15,16]. The 16k-point HyperSpeed FFT core from RFEL forms the central element of the system, performing the conversion from the time-domain to the frequency-domain, and it includes bit reversing to sort the data in natural frequency order. The FFT is built using a highly parallel architecture in order to achieve the very high data rate of 2 GBytes/s. The final step of processing contains the conversion of the frequency spectrum to a power representation and successive accumulation of these results. This accumulation step has the effect of averaging a number of power spectra, thereby reducing the background noise and improving the detection of weak signals. This step also reduces the huge amount of data produced by the earlier stages and eases any subsequent interface bandwidth requirements and processing loads. The output from the spectrometer core is in a 32-bit floating-point format. With an ordinary PC for further data-managing and data transfer, the FFTS is integrated into the APEX control network and interfaces with the control system APECS via SCPI commands, as described in[17].

### 3.3. FFTS: Frequency resolution

To understand the spectral resolution and effective channel bandwidth of the FFTS, the spectral leakage caused by the application of the Fourier Transform (FFT) to a noisy signal must be considered. Spectral leakage is the result of the assumption in the FFT algorithm that the signals are contained in a single FFT time record, and thus

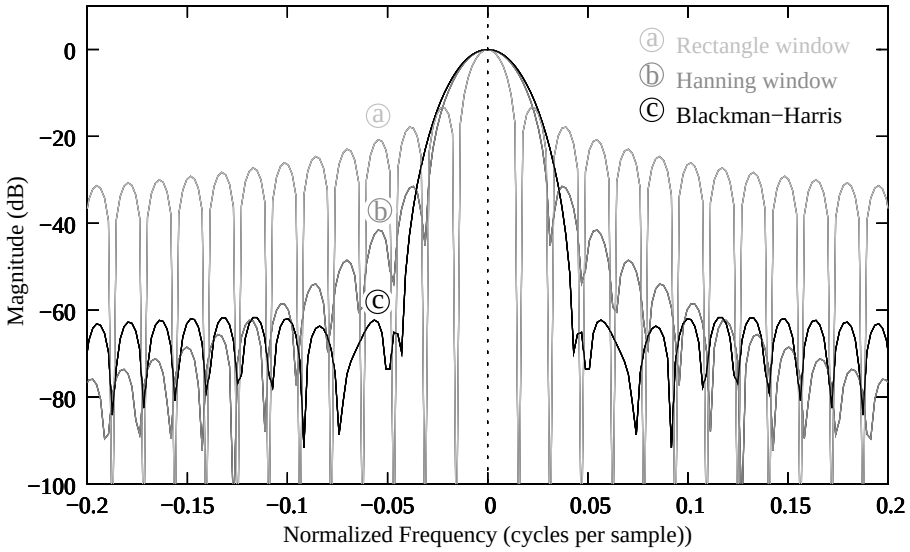


**Figure 6.** Comparison of two commonly used window functions for FFT weighting versus no (or rectangle) window application. Depending on the selected window, the frequency response of a single FFT bin varies in main-lobe, peak-sidelobe level and fall-off rate.

periodic at intervals corresponding to the length of this time record. If the time record has a non-integral number of cycles, this assumption is violated and spectral leakage occurs, which introduces a wide range of frequencies in the frequency domain and results in the energy of a signal spreading to adjacent frequency bins[15,16]. If no window function is applied prior to the FFT, the first sidelobes are attenuated by 13 dB relative to the main-lobe and the sidelobe fall-off rate is 6 dB per octave. Consequently, the selectivity of a bare FFT is poor, which results in a large amount of ripples in the passband. In addition, the spectral leakage from a large signal component may be so severe that other weaker signals at different frequencies are masked. The effects of spectral leakage can be restricted by reducing the discontinuities at both ends of the time record, i.e. by multiplying the data with a suitable window function. For radio astronomical applications a Blackman-Harris window is adequate due to its excellent spectral leakage attenuation and good amplitude conservation for random and noisy input signals. The APEX FFTS applies a 3-term Blackman-Harris window. Unfortunately, there is always a trade-off between the main-lobe width and the sidelobe leakage: As the sidelobe level decreases, the main-lobe width is increased (Fig. 6). To characterize this behaviour the equivalent noise bandwidth (ENBW) is usually used. The ENBW indicates the equivalent rectangular bandwidth of a filter with the same peak gain that would result in the same output noise power. Table 1 is a comparison of the properties of a rectangular, a Hanning and a Blackman-Harris window. Since the ENBW for a rectangle filter is 1.0, which is equal to the channel separation frequency (61.035 kHz), the frequency resolution for the APEX FFTS, applying the Blackman-Harris window, is 98.267 kHz.

**Table 1.** Comparison of window functions for FFT weighting

| Window function | highest sidelobe | fall-off rate | 3 dB BW (bins) | 6 dB BW (bins) | ENBW (bins) |
|---|---|---|---|---|---|
| Rectangle[a] | -13 dB | -6 dB/oct | 0.89 | 1.21 | 1.00 |
| Hanning[b] | -32 dB | -18 dB/oct | 1.44 | 2.00 | 1.50 |
| Blackman-Harris[c] | -61 dB | -6 dB/oct | 1.56 | 2.19 | 1.61 |

[a] $w(n) = 1$
[b] $w(n) = 0.5\,(1 - \cos(2\pi n/N))$
[c] $w(n) = 0.44959 - 0.49364\cos(2\pi n/N) + 0.05677\cos(4\pi n/N)$

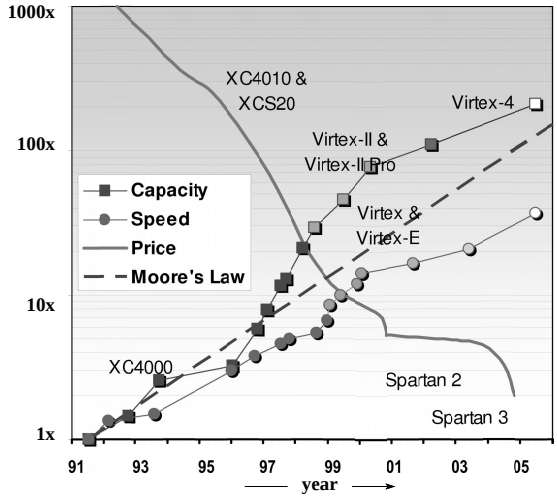


**Figure 7.** Moore's law for FPGAs: The diagram shows the continuous increase in complexity of FPGAs in terms of capacity and computing speed and the decrease of costs over the last 15 years. (reference: `www.xilinx.com`)

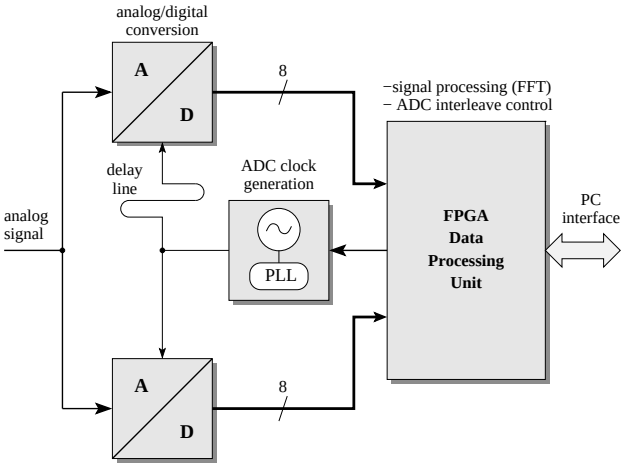


**Figure 8.** Functional diagram of two time-interleaved ADCs: Interleaving two ADCs is the process of using a second ADC with 180 degree phase-shift to fill data half way between the samples of the first ADC.

### 3.4. FFTS: Possibilities for future hardware and software improvements

From the astronomical community, there is a huge demand for flexible spectrometers with wider instantaneous bandwidth as well as relatively high spectral resolution. In addition, the upcoming heterodyne receiver arrays with up to a few hundred pixels require competitive spectrometers. In this regard only FFTS can offer perspectives (cp. Fig. 1).

The described APEX FFTS is limited by the maximum sampling rate of the ADCs for the achieved bandwidth and by the complexity of the FPGA chip for the spectral resolution. Although the APEX FFTS has been in operation for only one year, there are already much faster ADCs commercially available and the performance in terms of computing power of FPGAs has increased impressively. In Figure 7 we show the continuous increase of FPGA computing power over the last decade. With the recent announcement from XILINX that the first chips of the next generation of very complex FPGAs – the Virtex-5 family – are available, the performance of the fastest FPGA in Fig. 7 (Virtex-4) is again exceeded by a factor of ∼1.3. Also, the costs per processing unit decreased at a similar rate, thus making FFTS cheaper with time. The commercial interest on ADCs in the

**Table 2.** Monolithic A/D Converters, for $F_s \geq 1000\,\mathrm{MHz}$ and bits $\geq 6$

| Manufacturer | Part No. | Sample Rate | Channels | No. Bits | Input BW |
|---|---|---|---|---|---|
| Rockwell | RAD 004 | 4000 MHz | 1 | 6 | 6000 MHz |
| Atmel | AT84AS008 | 2200 MHz | 1 | 10 | 3300 MHz |
| Atmel | TS83102G0B | 2000 MHz | 1 | 10 | 3000 MHz |
| Maxim | MAX108 | 1500 MHz | 1 | 8 | 2200 MHz |
| National | ADC08D1500 | 1500 MHz | 2 | 8 | 1700 MHz |
| National | ADC081000 | 1000 MHz | 1 | 8 | 1700 MHz |
| National | ADC08D1000 | 1000 MHz | 2 | 8 | 1700 MHz |
| Atmel | JTS8388B | 1000 MHz | 1 | 8 | 2000 MHz |
| Maxim | MAX104 | 1000 MHz | 1 | 8 | 2200 MHz |
| Atmel | AT84AD001B | 1000 MHz | 2 | 8 | 1500 MHz |

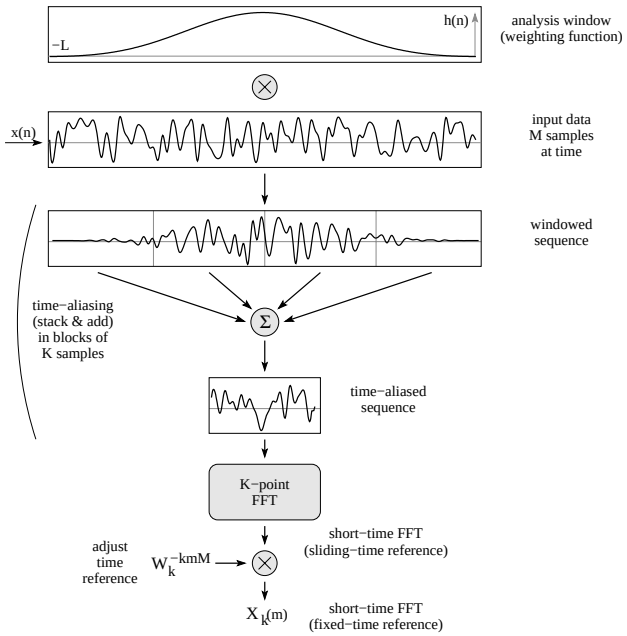


**Figure 9.** The Weighted Overlap-Add structure implements the Fourier transform filter-bank in terms of block-by-block analysis.

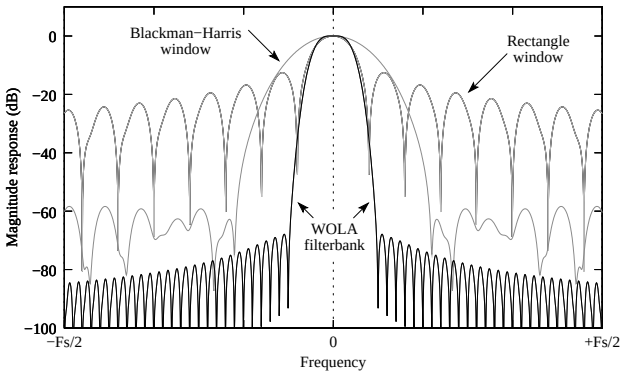


**Figure 10.** The frequency response of a single FFT bin is compared to an unweighted FFT (rectangle window), a Blackman-Harris window and to the WOLA method.

Giga-Hertz segment is mainly driven by applications such as wide-band satellite receivers, wireless RF infrastructures, instrumentation, aerospace, military and high energy physics. Furthermore the tremendous progress in the silicon process has led to ADCs with sample rates of 2 GHz and more. In Table 2 we compiled a list of the currently (05/2006) fastest commercially available ADCs. We direct the readers attention to the last column of Table 2, the analog input bandwidth of the ADC. This parameter, which limits the highest frequency that can be acquired, depends on the pace of the sample-and-hold circuit. For some of the ADCs in Table 2 the input bandwidth is twice the frequency of the sample rate, which makes this converter suitable for *time-interleaving*. Time-interleaving of ADCs means that the same analog signal is sampled with two or more ADCs applying phase-shifts in the respective sample clocks, thereby doubling (in the case of two ADCs) the coherent bandwidth in the sampling procress. Figure 8 illustrates the principle of interleave-sampling for two ADCs, which uses a 180 degree phase-shift between the ADCs to balance the sampling equally between the two ADCs. However, time-interleaving ADCs is not an easy task, since even when having perfectly linear components, gain/offset mismatches and phase errors may cause undesired spurs in the output spectrum. Gain and phase errors generate image spurs that show up at $F_s/2 - A_{\text{in}}$ ($A_{\text{in}}$ is the location of the analog input frequency in the first Nyquist zone). The offset spurs fall at the edge of the Nyquist band in the two-channel ADC system, but they may become a more serious problem for higher channel number systems. To overcome these distortion products it is necessary to apply high-precision correction techniques that hold their correction performance over wide bandwidths and temperature ranges. Since several of the correction approaches require adjustment of parameters best retrieved in the Fourier domain[18,19], time-interleaving within the FFTS can be implemented without additional processing requirements.

To clock the ADCs exactly 180° out of phase, it is possible to adjust the phase-shift by delay lines or by an adjustment of the clock's duty cycle if the ADCs samples in dual edge mode. For the FFTS application, we prefer a constant delay line attuned to the final sample frequency. The fine adjustment of the ADC interleaving can be done by changing the ADC clock frequency in a control-loop involved with the FPGA (Figure 8).

In future FFTS there is a request for the combination of wider instantaneous bandwidths by applying interleaved high-speed ADCs and the desired high spectral resolution results in spectra with many thousands of frequency channels. Of course, it is possible for these future FFTS to implement a FFT processing pipeline as described for the APEX FFTS in Sect. 3.2, but this has the slight disadvantage that the FFT has to be applied

**Table 3.** Hardware specifications of the ADC/FPGA board AC240

| | |
|---|---|
| ADC input sample rate | max 2 GS/s |
| ADC input bandwidth (-3 dB) | 0−1 GHz |
| ADC input resolution (quantisation) | 8 Bit |
| Maximum dynamic range (linear) | 48 dB |
| Input full scale range, selectable | -22 dB−16 dB |
| Ghost free dynamic range | >30 dB |
| FPGA Data Processing Unit | XILINX VirtexII Pro 70 |
| PCIbus interface | 32-bit, 33 MHz |

with an enormous number of data points, particularly if window weighting is necessary to achieve the required filter response (cp. Sect. 3.3). For instance, a 32k channel spectrum might require a window which is several 64K samples long. Such a window could be achieved by applying a FFT of this length and by decimating the output by a factor 2. But this approach would be very inefficient, especially since it would require parallel processing of several large FFTs.

Fortunately, a much more elegant and efficient method exists. Figure 9 shows the Weight Overlap and Add (WOLA) method in its most general form[20–22]. The required FFT filter response (Fig. 10) is determined by the weighting function $h(n)$, $0 \leq n < L$. To match the FFT length, the weighted data is separated into blocks of $K$ samples. The blocks are then added together, which corresponds to a *time-aliasing*, before a $K$-point FFT is applied. Fig. 9 also shows a post-FFT phase adjustment that compensates for the window's time origin. This adjustment is done by multiplying the FFT spectrum by $W_k^{-kmM}$. It is useful in applications where the phase of $X_k(m)$ is important. For the FFTS application this phase shift is of no relevance since the spectra will be integrated, and therefore this step can be skipped. Next, the input data are scrolled by M samples and the WOLA process is repeated. As implied in Fig. 9, the relationship between the length of the analysis window, the actual sample record and the FFT points is $M = L/K$. In the simple case of $M = K$, a new spectrum is obtained every $K$ samples. In this case, the system is referred to as *critically sampled*, i.e. the sample rate just satisfies the Nyquist criterion.

Although this processing method is adequate for many applications, one often requires some degree of oversampling to overcome aliasing problems, which are caused by critical sampling of a filter bank with finite cutoff rates. Within a WOLA filter bank this can be achieved by setting $M < K$, which results in an oversampling factor, $\xi = K/M$, greater than unity. The most attractive advantage of the WOLA method is that $\xi$ does not need to be an integer, thus the filter response of WOLA processing can be adjusted ideally to the application needs. In the case that $\xi$ is an integer, a different processing structure - usually referred to as *polyphase filter bank*[20] – may be used, which, for certain circumstances, can speed up the processing by requiring less memory with the trade-off of less flexibility.

In case of critical decimation, the only difference between the WOLA and polyphase filter bank is the order of the operations. The polyphase structure is data point oriented, which means each new data point is filtered by its corresponding polyphase filter and then Fourier transformed. The WOLA structure is block oriented, thus it first accumulates a block of data, then separates it in into segments, adds the segments and finally performs the Fourier transform.

In summary, we have shown the considerable potential of FFTS in future spectrometer developments, supported by the commercial interests in high-speed ADCs and the continuously increasing performance of FPGAs. Applying time-interleaved ADCs and WOLA or polyphase techniques to increase both bandwidth and the FFT filter performance, we intend to push FFT spectrometers to a few GHz bandwidth with spectral resolution of a few tens of kHz in the near future.

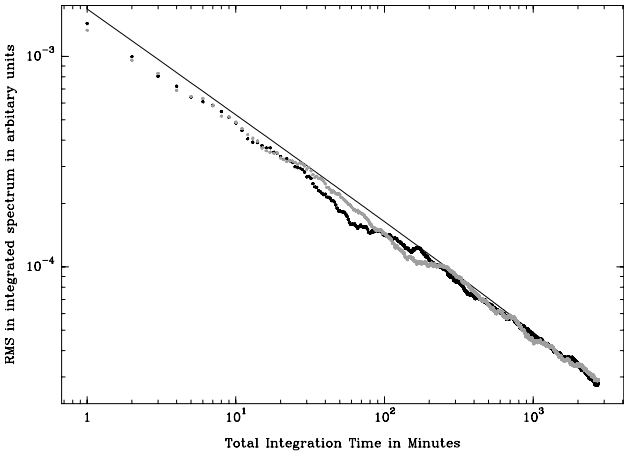


**Figure 11.** Decrease of noise in accumulated spectra (60 sec/dump) vs. total integration time, as measured with a noise diode. Both IF channels of the FFTS are plotted (in black and grey), for comparison the expected slope $1/\sqrt{t_{\rm int}}$ is given.

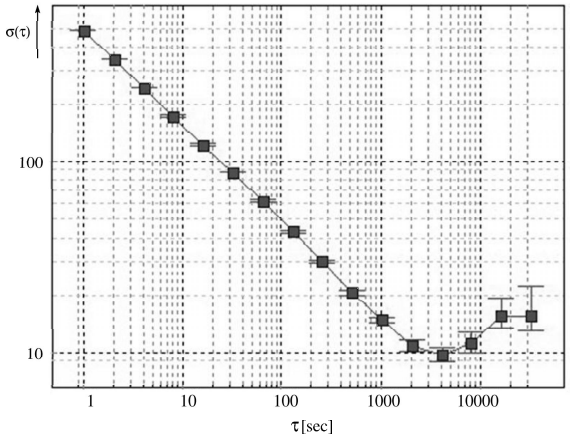


**Figure 12.** The remarkable stability of the APEX FFTS is illustrated in this Allan-Variance-Plot. The spectrum of a noise source (0-1 GHz) was integrated and processed in the FFTS. The spectroscopic variance between two 1 MHz broad channels, separated by 600 MHz within the band, was determined to be stable on a timescale of $\sim 4000$ s.

**Table 4.** Specifications of the FPGA/FFT-processing pipeline

| | |
|---|---|
| Fast Fourier Transform (FFT) | RFEL, HyperSpeed FFT |
| FFT - number of frequency channels | 16384 |
| FFT - channel separation | 61.035 kHz |
| FFT - Blackman-Harris window | 3 term, -61 dB sidelobe |
| FFT - frequency resolution | 98.267 kHz |
| FFT - arithmetic | 2's complement, 18-bit |
| Digital Half Band Filter (DHBF) | 50−950 MHz |
| DHBF - Stopband rejection | +48 dB |
| DHBF - Passband ripple | max ±0.1 dB |
| Power spectra builder (sum of squares) | full precision, 33-bit |
| On-board accumulation (integration) | 54-bit precision |
| Integration - max time (full precision) | ∼35 s |
| Integration - min time | 32.768 $\mu$s |
| Stability/Allan-Variance: only FFTS | $\sim$ 4000 s (Fig. 12) |

## 4. SPECIFICATION AND PERFORMANCE OF THE ACTUAL APEX FFTS

In Tables 3 and 4 we compile the specifications and the achieved performance of the APEX FFTS, its ADC/FPGA board and the FPGA/FFT-processing pipeline. To illustrate the performance we plot in Figures 11 and 12 the results of stability tests, performed pre-shipment at MPIfR.

Figure 11 presents the continuous decrease of the accumulated noise vs. integration time, which followed the radiometer formula, i.e. $\propto 1/\sqrt{t_{\rm int}}$, for nearly two days of operation. Figure 12 displays an Allan-Variance plot of the spectrometer using a temperature stabilized noise source, emphasizing the remarkable stability of the FFTS, on a timescale of $\sim 4000$ s.

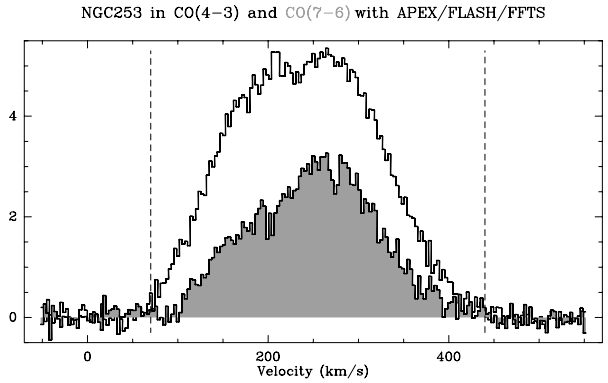


**Figure 13.** Spectra of warm carbon monoxide towards the nucleus of NGC 253, observed with the FLASH receiver at APEX.[23] The emission of CO(4–3) (at 461 GHz, top line), observed with 1 GHz bandwidth, is superimposed on the CO(7–6) line (806 GHz). The latter has been observed with an effective bandwidth of 1.8 GHz (composed of two 1 GHz bands, offset by 800 MHz). The dashed vertical lines indicate the bandwidth of 1 GHz for the CO(7–6) line. Clearly, the velocity width is barely sufficient to define the zero level (baseline), emphasizing the need for wide bandwidth spectrometers for extragalactic work at submm frequencies.

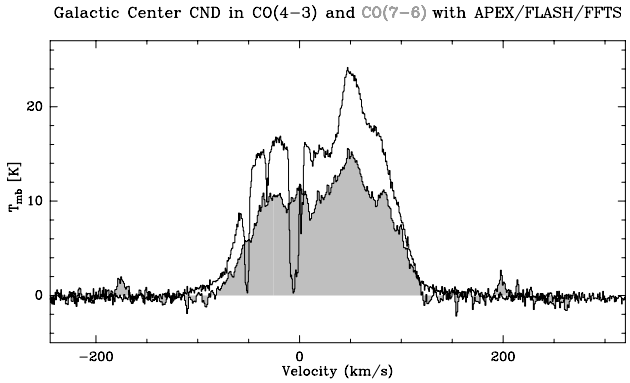


**Figure 14.** Spacially averaged CO spectra towards the innermost ± 30 arcsec of the Galactic Center, observed with FLASH. The emission of CO(4–3) (top spectrum), observed with 1 GHz bandwidth, is superimposed on the CO(7–6) line (filled grey) observed with 1.6 GHz bandwidth - no baseline-fitting applied to these spectra. Clearly the prominent broad CO emission is visible, but also narrow absorption lines and high velocity emission features with velocities up to 200 km/s can be identified. These spectra clearly show the advantage of having a wide spectral coverage with high resolution, allowing for simultaneous observation of a broad emission spectrum and relatively narrow line-of-sight absorptions.

## 5. OBSERVATIONAL EXAMPLES

Because in many astronomical objects the intrinsic velocity structure is independent of frequency, while the frequency width scales linearly with the observed line frequency

$$\Delta f = f_{line} \frac{\Delta v}{c} \tag{1}$$

observations at submm frequencies require spectrometers with increasingly wider bandwidths to allow for a complete coverage of the full line width of the observed object in one exposure.

In Fig. 13 we show the spectra of warm carbon monoxide towards the starburst nucleus of the galaxy NGC 253 as observed with APEX. Clearly, with an actual line width of more then 300 km/s, a spectrometer bandwidth of only 1 GHz is insufficient to study the emission of CO(7–6) at 806 GHz. However, by combining two 1 GHz wide spectrometers, offset in their IF center frequencies by 800 MHz, it was possible to observe the complete emission with sufficient baseline in a single integration, thus avoiding problems of cross-calibration, pointing errors, and platforming effects of otherwise sequential observations.

Even more demanding are observations of regions with complex kinematics like the molecular gas in the center of our Galaxy. Emission from several distinct velocity components in the inner 10 pc of our Galaxy combine into rather complex spectra, all blended by narrow absorption features from lower excitation gas along this line-of-sight. To disentangle these structures (in velocity space) high spectral resolution with wide velocity coverage is absolutely necessary. In Fig. 14 we display two spectra of warm carbon monoxide towards the central ± 30 arcsec of the Galactic Center. Prominently seen is the broad carbon monoxide emission, resulting partly from the prominent circumnuclear disk orbiting about the central mass condensation. Narrow absorption features, some of them narrower then 10 km/s, originate from gas along the line-of-sight that is the innermost gas concentration. The excitation of this gas is too low to absorp CO(7–6) photons, but absorption is nicely seen from the lower J=3 level.

These examples highlight the advantages of wide-band spectrometers with high spectral resolution, when studying objects with such complex velocity structure. Another example of a rather different observational application are line surveys. Line surveys are a powerful tool for investigating the chemical and physical structure of molecular clouds and starforming regions. While the individual lines are relatively narrow, a wideband spectrometer with good velocity resolution will allow one to cover as many lines as possible in one single exposure, thus increasing the observing efficiency with enhanced calibration quality.

In summary, it is obvious from an observational point of view that the large number of spectral channels achievable with FFT spectrometers eliminates the disadvantage and complexity of autocorrelator systems that have to reduce the bandwidth to get higher spectral resolution. Therefore FFT spectrometer are better suited for combined broad band and high resolution observations.

## 6. CONCLUSION

As discussed before, radio astronomical heterodyne observations require spectrometers that provide both wide bandwidth coverage and high spectral resolution, thus large number of spectral channels. There are potential advantages of FPGA-based FFT spectrometer that favour the FFTS in comparison to other spectrometers for these radio astronomical applications:
The FFTS provides an instantaneous high bandwidth of 1 to a few GHz in the future with up to 16k spectral channels (32k channels in preparation at MPIfR) in a single FPGA chip, that simplifies various observations by avoiding e.g. problems of cross-calibration or platforming and increasing observing efficiency. Due to the full 8-bit signal sampling no additional calibration by means of implicit total power measurements are required. In consequence a higher sensitivity and stability compared to that of autocorrelators and acousto-optical spectrometers can be achieved. In addition, this multi-bit sampling provides a higher dynamic input-range, so a less sophisticated autogain control is needed. Consequently, the IF processor is less complex, making the system more stable. Another reason for the very high system stability of FFTS is the pure digital signal processing.
The FFTS has been in routine operation since May 2005 at the APEX. The backend has been proven extremely reliable and robust, even under the harsh environmental conditions at this remote facility. For this aspect of operation it is also an advantage that the FFTS requires little space and low power, thus it is safe also for use at high altitude sites (e.g. APEX at 5100 m) as well as on satellites.
And finally the low price compared to traditional spectrometers through use of commercial parts and the modular design with calibration-free digitizer / analyzer boards, thus the simple reproducibility, makes the FFTS also attractive for multi-band applications, e.g. for multicolour[23] and / or array receivers[24,25].

To summarize, our novel FPGA-based FFTS development offers exciting perspectives for high-resolution broadband spectrometers. In addition, as outlined before, even the existing system may be improved by progresses in the software. Beside this, the new class of high-speed ADCs and the advantages of FPGA, with their wide availability, decreasing costs (both based on the large commercial interest) and increasing processing capability (Moore's Law), make it very likely that FFTS can be pushed to broader bandwidths in the near future.

## REFERENCES


1. R. Güsten, L.-Å. Nyman, P. Schilke, K. M. Menten, D. Cesarsky, and R. Booth, "The Atacama Pathfinder EXperiment Telescope," *A&A, in press* , 2006.
2. J. Horn, O. Siebertz, F. Schmülling, C. Kunz, R. Schieder, and G. Winnewisser, "A 4 x 1 GHz Array Acousto-Optical Spectrometer," *Experimental Astronomy* **9**, pp. 17–38, 1999.
3. R. T. Schieder, O. Siebertz, C. Gal, M. Olbrich, F. Schloeder, R. Bieber, F. Schmuelling, V. Tolls, and J. M. M. Horn, "Toward very large bandwidth with acousto-optical spectrometers," in *Millimeter and Submillimeter Detectors for Astronomy. Proceedings of the SPIE, Volume 4855*, T. G. Phillips and J. Zmuidzinas, eds., pp. 290–300, Feb. 2003.

4. P. Hartogh, "Present and future Chirp transform spectrometers for microwave remote sensing," in *Sensors, Systems and Next-Generation Satellites, SPIE Proc 3221, SPIE, Washington*, H. Fujisada, ed., pp. 328–339, 1997.
5. G. Villanueva and P. Hartogh, "The high resolution chirp transform spectrometer for the SOFIA-GREAT instrument," *Experimental Astronomy* , pp. 1–15, May 2006. Springer Netherlands.
6. G. Villanueva, "The High Resolution Spectrometer for SOFIA-GREAT," *PhD thesis* , Nov. 2004. University of Freiburg.
7. S. Weinreb, "A digital spectral analysis technique and its application to radio astronomy," *Technical Report* **412**, 1963. Research Lab Electronics, MIT, Cambridge, USA, `http://hdl.handle.net/1721.1/4413`.
8. W. Wiedenhöver, "MACS – the MPIfR Array Correlator System," *MPIfR Technical Report* , 1998.
9. L. Ravera, P. Cais, M. Giard, A. Baudry, D. Lagrange, G. Montignac, J. L. Noullet, E. Caux, A. Cros, J. M. Desbats, J. B. Begueret, D. Navarro, and N. Lavigne, "Wideband high-resolution versatile spectrometer proposed for FIRST-HIFI," in *Proc. SPIE Vol. 4013, UV, Optical, and IR Space Telescopes and Instruments*, J. B. Breckinridge and P. Jakobsen, eds., pp. 305–312, July 2000.
10. A. Harris, "Spectrometers for Heterodyne Detection," in *Proc. of the FarIR, SubMM, and MM Detector Technology Workshop*, J. Wolf and J. Davidson, eds., 2002.
11. A. I. Harris, "Heterodyne spectrometers with very wide bandwidths," in *Millimeter and Submillimeter Detectors for Astronomy. Edited by Phillips, Thomas G.; Zmuidzinas, Jonas. Proceedings of the SPIE, Volume 4855, pp. 279-289 (2003).*, T. G. Phillips and J. Zmuidzinas, eds., pp. 279–289, Feb. 2003.
12. S. Stanko, B. Klein, and J. Kerp, "A field programmable gate array spectrometer for radio astronomy. First light at the Effelsberg 100-m telescope," *A&A* **436**, pp. 391–395, June 2005.
13. B. Klein, S. D. Philipp, I. Krämer, C. Kasemann, R. Güsten, and K. M. Menten, "The APEX Digital Fast Fourier Transform Spectrometer," *A&A, in press* , 2006.
14. A. O. Benz, P. C. Grigis, V. Hungerbühler, H. Meyer, C. Monstein, B. Stuber, and D. Zardet, "A broadband FFT spectrometer for radio and millimeter astronomy," *A&A* **442**, pp. 767–773, Nov. 2005.
15. F. J. Harris, "On the Use of Windows for Harmonic Analysis with the Discrete Fourier Transform," *Proceedings of the IEEE* **66**, pp. 51–83, 1978.
16. A. H. Nuttall, "Some Windows with Very Good Sidelobe Behavior," *IEEE Trans ASSP* **29**, pp. 84–91, 1981. (Includes corrections and additions to Harris 1978).
17. D. Muders, H. Hafok, F. Wyrowski, E. Polehampton, A. Belloche, C. König, R. Schaaf, F. Schuller, J. Hatchell, and F. v.d.Tak, "APECS - The Atacama Pathfinder Experiment Control System," *A&A, in press* , 2006.
18. N. Kurosawa, H. Kobayashi, K. Maruyama, H. Sugawara, and K. Kobayashi, "Explicit analysis of channel mismatch effects in time-interleaved ADC systems," *Circuits and Systems I: Fundamental Theory and Applications, IEEE Transactions* **48**, pp. 261 – 271, 2001.
19. T.-H. Tsai, P. J. Hurst, and S. H. Lewis, "Time-Interleaved Analog-to-Digital Converters for Digital Communications," in *The IASTED Conference on Circuits, Signals, and Systems*, M. H. Rashid, ed., 2004.
20. R. E. Crochiere and L. R. Rabiner, *Multirate Digital Signal Processing*, Prentice Hall, 1983. ISBN 0-13-605162-6.
21. J. Lillington, "Slice and Dice Chunks of Radio Spectrum," *Wireless Systems Design* **8**, p. 39, Nov. 2003. ISSN 1089-5566.
22. C. C. Gumas, "Window-presum FFT achieves high dynamic range, resolution," *Personal Engineering & Instrumentation News* , pp. 58–64, July 1997. `www.chipcenter.com/dsp/DSP000315F1.html`.
23. S. Heyminck, C. Kasemann, R. Güsten, G. de Lange, and U. U. Graf, "FLASH - The first light APEX Submillimeter Heterodyne instrument," *A&A, in press* , 2006.
24. R. Güsten, G. A. Ediss, F. Gueth, K. H. Gundlach, H. Hauschildt, C. Kasemann, T. Klein, J. W. Kooi, A. Korn, I. Kramer, H. G. Leduc, H. Mattes, K. Meyer, E. Perchtold, and M. Pilz, "CHAMP: the Carbon Heterodyne Array of the MPIfR," in *Proc. SPIE Vol. 3357, p. 167-177*, T. G. Phillips, ed., pp. 167–177, July 1998.
25. C. Kasemann, R. Güsten, S. Heyminck, B. Klein, T. Klein, and S. D. Philipp, "CHAMP+: a powerful sub-mm array for APEX," in *Millimeter and Submillimeter Detectors and Instrumentation for Astronomy III. Proc. SPIE, Vol. 6275, in preparation*, 2006.